P and R wave detection in complete congenital atrioventricular block

J. GUERRERO,[1] M. MARTÍNEZ,[1] R. MAGDALENA,[1] J. MUÑOZ,[1] M. BATALLER,[1] A. ROSADO,[1] J.V. FRANCÉS,[1] J. CHORRO[2]

[1] Digital Signal Processing Group, Department of Electronic Engineering, University of Valencia, 46100 Dr. Moliner, 50, Burjassot (Valencia), Spain;

[2] Service of Cardiology, University Clinic Hospital, Avda. Blasco Ibañez 17, 46010, Valencia, Spain

Abstract

Complete atrioventricular block (type III AVB) is characterized by an absence of P wave transmission to ventricles. This implies that QRS complexes are generated in an autonomous way and are not coordinated with P waves. This work introduces a new algorithm for the detection of P waves for this type of pathology using non-invasive electrocardiographic surface leads.

The proposed algorithm is divided into three stages. In the first stage, the R waves located by a QRS detector are used to generate the RR series and time references for the other stages of the algorithm. In the second stage, the ventricular activity (QT segment) is removed by using an adaptive filter that obtains an averaged pattern of the QT segment. In the third stage, a new P wave detector is applied to the residual signal obtained after QT cancellation in order to detect P wave locations and get the PP time series.

Eight Holter records from patients with congenital type III AVB were used to verify the proposed algorithm. Although further improvements should be made to improve the algorithm's performance, the results obtained show high average values of sensitivity (90.52 %) and positive prediction (90.98%).

Keywords

Complete congenital atrioventricular block, P and R wave detection, QRS, adaptive impulse correlated filter, SNEO.

Introduction

An atrioventricular block (AVB) is a cardiac pathology in patients with deficient conduction in the atrioventricular system (AV) and His-Purkinje bundle. Depending on its intensity, the block is classified in three grades: I, II and III. Type I AVB is characterized by a PR elongation above 0.2 seconds (typical duration is considered to be between 0.12 and 0.2 seconds). Electrophysiological studies have determined that type I AVB is caused by a delay in the AV node conduction or in the His-Purkinje bundle, or in both. Type II AVB is characterized by failures in the cardiac conduction system causing some P waves not to be transmitted; therefore, QRS complex is not generated. In type II pathology, the PR segment gets longer and longer until the P wave fails to appear. Type III AVB implies a total absence of conduction in the AV system. There is no transmission to the ventricles for P waves, and the QRS complexes are generated in an autonomous way that is not coordinated with P waves [6] (Figure 1).

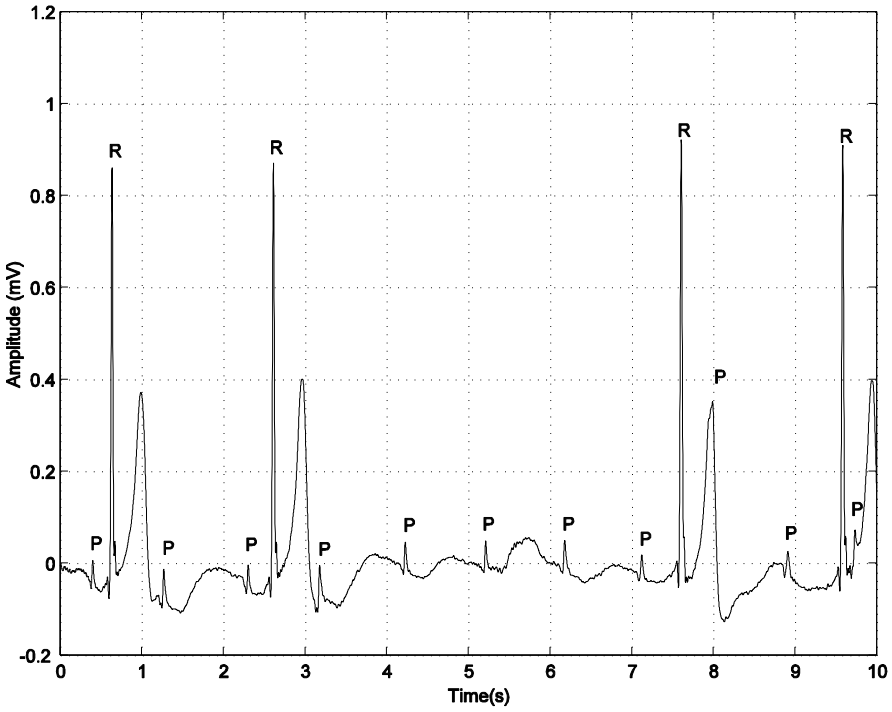

Figure 1. Electrocardiographic signal showing type III AVB. R and P annotations show the R wave and the P wave, respectively.

This type III AVB can be acquired or congenital. When it is acquired, it might appear after a heart attack, medical intoxication, or other factors [21, 26]. Congenital complete atrioventricular block has an

incidence of 1 in 20,000 live born infants [19]. During childhood some children are asymptomatic, but most of the patients need implantable pacemaker therapy when they are adults [20].

In this pathology, the activity of secondary pacemakers is modulated by extrinsic factors. The analysis of the ventricular rate variability permits the study of the mechanisms implied in its control [3, 11]. If both, atrial and ventricular rhythms are known (PP and RR series), the analysis of atrial rate variability and its relationships with ventricular variability can be studied for this pathology.

There are few works on detecting auricular activity in type III AVB, due to its low incidence [19]. In this pathology, P wave and QRS-T generation are independent [9, 24]. Therefore, P-wave detectors based on relative positions between R and P waves cannot be used [13, 25, 27]. Esophageal or intracavitarial electrodes have been used to obtain an isolated atrial activity that allows the P wave [11] to be detected. When non-invasive electrocardiographic surface leads are used (as in Holter records), other techniques such as pattern detection fail when the P wave is overlapped with the QRS complex or the T wave [10].

From the point of view of signal processing, the detection of atrial activity in type III AVB is similar to the problem of extracting the fetal ECG (FECG) from non-invasive abdominal records. In FECG, maternal and fetal heart electrical activities are independent, and the objective is usually to detect the R wave in the FECG signal. Techniques such as blind separation sources (BSS) or independent component analysis (ICA) have been applied to this problem [32]. Another approach is to cancel the unwanted contribution of the signal, obtaining the residue signal. In FECG, the unwanted signal is the maternal ECG; in type III AVB, the unwanted signal is the ventricular activity). Then the desired component can be detected. Adaptive filtering [7], subtraction of an abdominal maternal averaged pattern [1] as well as mixed techniques [16, 18 8] have been applied.

The aim of this work is to develop a P wave detector for type III AVB using non-invasive electrocardiographic surface leads. The paper is structured as follows; section 2 describes the ECG records used for the analysis and the methodology for the proposed algorithm. Section 3 shows the method used for QT cancellation. Section 4 shows the P wave detector. Section 5 reports the obtained results, and finally, section 6 states the conclusions.

Materials and methods

Patients and acquisition

For this study, eight Holter records from patients with congenital type III AVB were used. These records were obtained from several local hospitals and are protected under the Spanish data protection law. Their ages ranged from 3 to 36 years (mean: 13, standard deviation: 10). All the records had narrow QRS escape rhythms. No cardiac anatomical malformations associated with AVB were detected, no cardioactive drug treatment was administered, and no pacemakers were implanted.

The cardiac signal was recorded using Tracker and SpaceLabs Medical magnetic recorders. The records were 24 hours long (mean: 26.06, std. dev.: 0.82). The recorded tapes were read using a Pathfinder II (Reynolds Medical, Irvine, CA) analyzer connected to an acquisition board ICPDAS 1202 (ICPDAS Co., Taiwan). Signals were sampled with 12-bit resolution at a sampling rate of 1kHz [3]. Two leads were acquired for every record. However, in this work the algorithm was applied to the best signal-to-noise ratio (SNR) lead, which was determined by visual inspection. The data were divided into estimation (training) and evaluation (testing) sets, containing four records each one.

Proposed algorithm

P wave detectors usually use the relationship between the P wave and the QRS complex during normal cardiac rhythm [13, 25, 27], applying a search window to the left side of the QRS complex. However, since atrial and ventricular activities are not related in type III AVB, the P and the R waves are not related, either. Thus, P waves might be overlapped with QRS or T waves, and, a traditional P wave detector cannot be used in this case.

The proposed method detects P waves in the residual signal obtained from the cancellation of the ventricular activity (QT segment). As mentioned above, this approach has been used for maternal ECG cancellation in abdominal fetal electrocardiogram records [1] where a maternal averaged pattern is obtained

from the abdominal signal by using an appropriate reference signal. This way the maternal contribution is removed and the residual signal is obtained. The residual signal contains mainly fetal contribution, and fetal QRS complexes can be located with an appropriate algorithm. The method proposed is analogous: the QT segment would be related to maternal contribution, and the P waves would be related to fetal QRS complexes.

The proposed stages to obtain the RR and PP series in type III AVB records are the following (see Figure 2):

1) The record is divided into segments; every segment is *t_segm* duration. After segmentation, the segments are pre-processed.
2) A QRS detector is used for R wave positioning in the pre-processed signal. R wave positions are used by the QT pattern canceller to locate the pulses to be averaged. They are also used by the P detector to locate the QRS residues. Furthermore, the R detector provides the RR time series.
3) After QT segment cancellation, the residual signal is obtained. The P wave is localized in the residual signal using a P detector, and the PP time series is calculated.

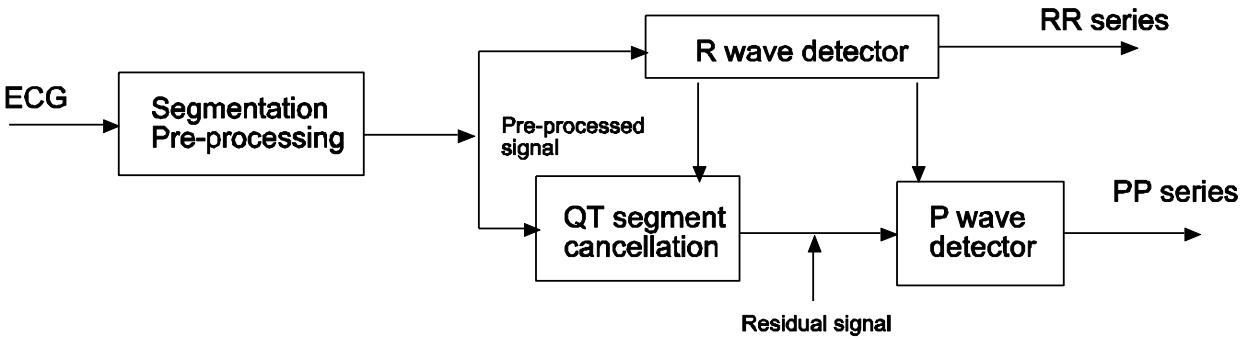

Figure 2. Block diagram for the proposed algorithm.

Let us describe each module.

Preprocessing.

As a previous stage for the P wave detector, all the records are pre-processed in order to eliminate baseline wander and power line interference. An interpolated finite impulse response (FIR) filter with lineal phase

was used to extract these kinds of interferences [30]. The output of the filter is subtracted from the original signal to cancel the interferences.

R wave detector.

A QRS detector proposed by Pan and Tompkins [23] and modified by Laguna [17] was used. The detector is based on an adaptive threshold in the ECG amplitude that has been previously filtered with a band-pass filter (12-22 Hz).

QT pattern cancellation

The procedure implemented for QT pattern cancellation is called Adaptive Impulse Correlated Filter (AICF), which was proposed by Thakor [29] and used by Laguna [16] and Almenar [2] for repetitive component detection in ECG, and removal of the maternal ECG component in a fetal ECG [18]. Another cancellation technique like the one described by Stridh [28] cannot be used because it needs three leads.

The AICF algorithm is based on the periodic nature of ECG. Therefore, averaging techniques are used to perform a noise reduction. As the cardiac rhythm is not constant, some references are needed for pulse averaging. These references are generated from the QRS complex detector. Figure 3 shows a block diagram for the proposed QT segment cancellation. The AICF is an adaptive filter [31] that is based on the Least Mean Square algorithm (LMS) where the desired signal (here called pre-processed signal), *d(n)*), is obtained after the pre-processing stage. The reference signal, x(n), for this adaptive filter structure uses a 0 value sequence except in specific samples called regeneration times [7] where the value is 1. Regeneration times are located at a fixed number of samples (*La*) before the QRS. A different method [2] includes a delay block of *La* samples in the *d(n)* signal before the subtraction of the adaptive filter output signal (*y(n)*), which is equivalent to the proposed method here. Thus, the regeneration times are placed in the positions given by the QRS complex detector.

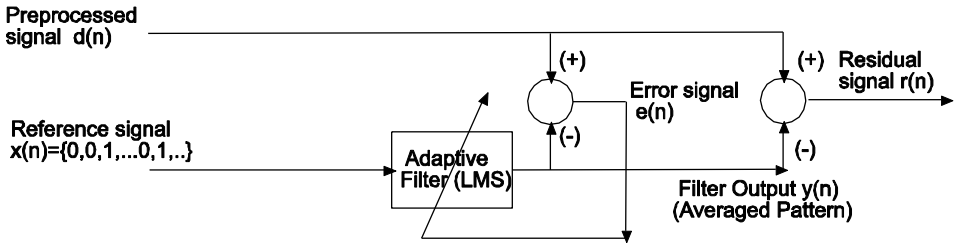

Figure 3. AICF algorithm structure for the QT pattern cancellation.

The proposed adaptive filter behaves like an exponential averager. The adaptive filter coefficients store an averaged version of the signal [16]. The adaptive filter length is essential for this application because the averaged pattern is the signal that begins with the regeneration times and has a length that is equal to the filter length. Obviously, the filter length must be lower than the RR interval so that no overlapping between ECG pulses exists.

The adaptive filter output, *y(n)*, is subtracted from the original signal in order to cancel the contribution of the existing QT segment. In the AVB pathology, P waves have an independent rhythm; therefore, the averaging process will attenuate such waves in the pattern (they will appear in different positions, depending on the pulse) and will improve the SNR of the subjacent signal, the QT segment. The process is similar to coherent averaging of QT segments, where the segments are averaged by using the QRS complex as reference. This method reduces the noise by a factor of $\sqrt{N}$, with N being the number of averaged QT segments [15]. One of the main advantages of the AICF is the fact that it behaves like an exponential averager, so slow variations in the signal are retained, and thus a better cancellation is obtained.

Since the cancellation algorithm is based on pattern subtraction, the location and correct pattern alignment before performing the subtraction is decisive for the algorithm's performance. The sampling rate also plays an important role. Pattern subtraction techniques provide the best results when the sampling rate is high. For this reason, a 1-kHz sampling rate is used, reducing the low-pass filter effect due to the presence of alignment errors [12]. This fact affects the remaining QT segment contribution in the *r(n)* signal, which is not only influenced by the correct alignment of QRS pulses, but also by the selected value for the adaptation constant (μ) in the adaptive algorithm.

Choosing the length and the starting point of the pattern to cancel**.**

The parameters to be defined are the starting point and the length of the pattern to be cancelled. This parameter will set the regeneration times and, therefore *x(n)*. The ends of the QT interval will be automatically determined taking into account the particular characteristics of each record. The procedure is the following:

i. The RR series is calculated in the segment under study.

ii. The average heart rate *RRav* is calculated (the averaged heart rate of the records under study is 45±8 beats per minute

iii. The length of the pattern is calculated as $L = Lqrs + Lt$, with $Lqrs = 151\,ms$ and $Lt = \left(0.47 \cdot \sqrt{RRav}\right) \cdot 1000$, with RRav being the average heart rate, (in seconds) of the studied segment. This value takes into account the normal values of the QRS complexes (0.12s) [24] which is increased by 0.03 s in order to include isoelectric segments of the ECG. The length of the T-wave takes into account the normal values of the QT segment, which for a heart rate of about 40 beats per minute is 0.49 s in this pathology [24].

iv. The reference signal *x(n)* is generated by positioning the regeneration times 75 ms before the location of the R wave marked by the QRS detector.

Figure 4 shows a segment of the signal *d(n)* and the signal *x(n).* Both signals are the inputs of the proposed adaptive structure. The segment marked with an arrow (*L* samples) is the one taken into account during the process of updating the weights of the adaptive filter. These segments will be exponentially averaged in accordance with the behavior of the algorithm, and the result will be stored in the adaptive filter weights.

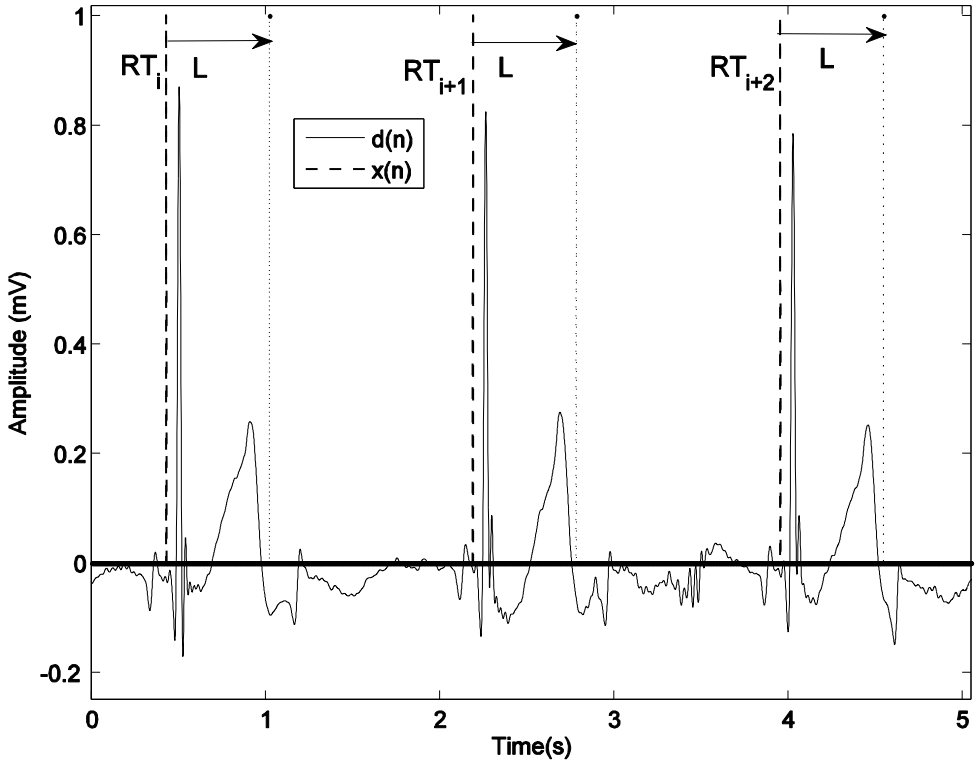

Figure 4. Regeneration times (RT) and length of the adaptive filter (L) for QT segment cancellation

Pattern subtraction.

The process of subtracting the output of the adaptive filter (*y(n)*) from the original signals can generate discontinuities in the first and last sample of the pattern, since segments of the filter output are equal to zero but their value in the original signal can be different from zero (segments between samples RT_i+L and RT_{i+1} in Figure 4). In order to avoid this effect, a linear interpolation in *y(n)* signal is performed between the end of a pulse and the beginning of the next pulse. Figure 5 shows the diagram of the process. Figure 5a shows the pre-processed signal *d(n)* and the reference signal *x(n)*. Figure 5b shows the output of the filter *y(n),* which contains an averaged pattern. This figure shows segments (marked with arrows) in which the output of the filter is zero. Figure 5c shows the residual signal: the dotted line ($r_{nc}(n)$) indicates that the signal is obtained by direct subtraction, when the discontinuity can be noted; and the solid black line ($r_c(n)$) indicates the resultant signal when linear interpolation is applied between consecutive pulses.

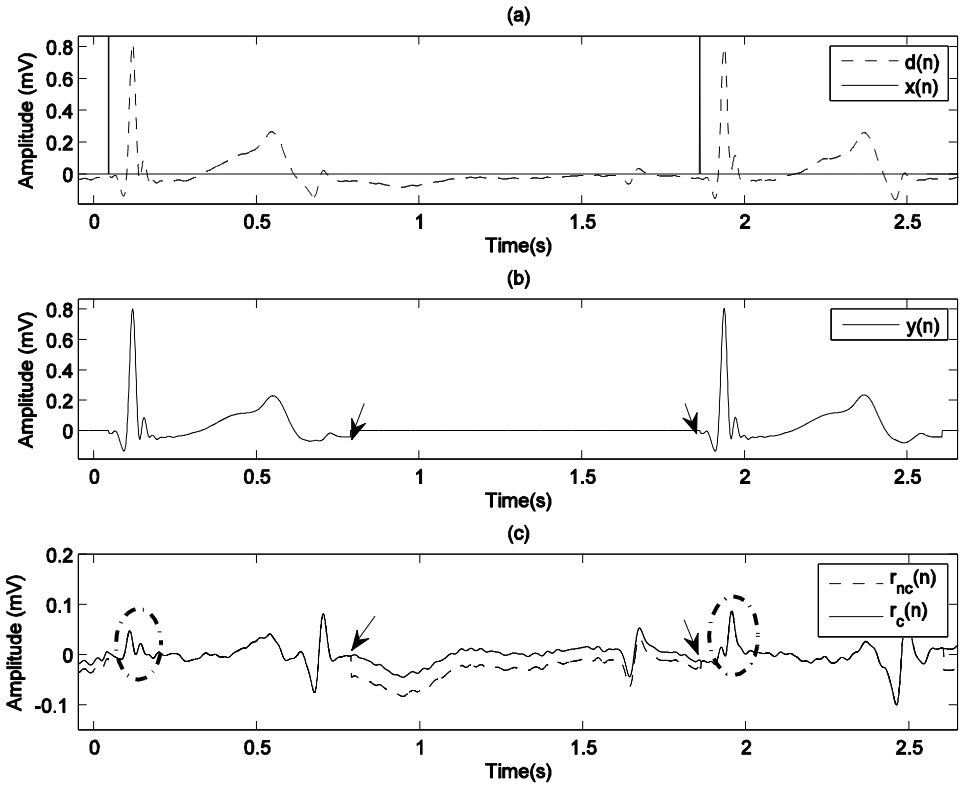

Figure 5. These figures show the effect of subtracting the output of the adaptive filter: (a)This figure shows the pre-processed signal (d(n))and the reference signal (x(n)); (b) This figure shows the output of the filter, in which the arrows mark the segments in which the output is zero; (c)This figure shows the residual signal: discontinuous line ($r_{nc}(n)$) without interpolation, and continuous line $r_c(n)$ performing a linear interpolation between the end of a pulse and the beginning of the next one prior to cancellation. The QRS residues are shown inside the ovals

Selection of the constant of adaptation.

The algorithm used to update the weights of the adaptive filter is the classical LMS, in which the adaptation constant controls the speed of convergence and the stability of the system [5]. An simple explanation of the application of this algorithm to remove noise in cardiovascular signal can be found in [4]

In our case, the adaptation constant controls the depth of the average, that is, the contribution of the latest pulses. Since the repetitive component must be cancelled, a linear averaging of the pulses would provide the greatest improvement in the SNR. However, this method requires enormous memory capacity to store all the pulses, and the capability of adaptation to changes in the input signal would be lost. Another

possibility would be to use exponential averaging. In this case, high values of the constant give greater importance to the latest pulses, so not only the repetitive component will be cancelled but also the P waves. Therefore, the selection of this constant is of great importance.

Since the pulse to be cancelled contains the QT segment, but the alignment is performed based on the peak of the R wave, some alignment problems may arise on T wave. This has led the authors to consider different alternatives to determine the optimal adaptation constant, which will be explained in section 5. Another aspect to be taken into account is to determine whether the selected constant can be used to process the whole record or if it must be modified, since the files are very long.

P wave detection

Preprocessing

The residual signal obtained after the cancellation of the QT pattern is mainly composed by the P waves and the residues of the QT segment cancellation (in which the QRS residues sometimes show amplitudes that are equal to or greater than the P waves (Figure 6b)). In order to improve the signal-to-noise ratio on P waves, a preprocessing of the residual signal is performed to reject the superimposed noise and to minimize the effect of cancellation limitations of ventricular activity. Based on the spectral analysis of the signal, the presence of frequency components above 15Hz are mainly due to QRS residues, while components below 5Hz come from the contribution of baseline wander and T wave residues. Therefore, in our study, a fourth-order Chebysev type II band pass filter (5-15 Hz) was designed and applied. Then, a zero-phase forward and reverse digital filtering was performed, so the effective order was 8th (Figure 6c).

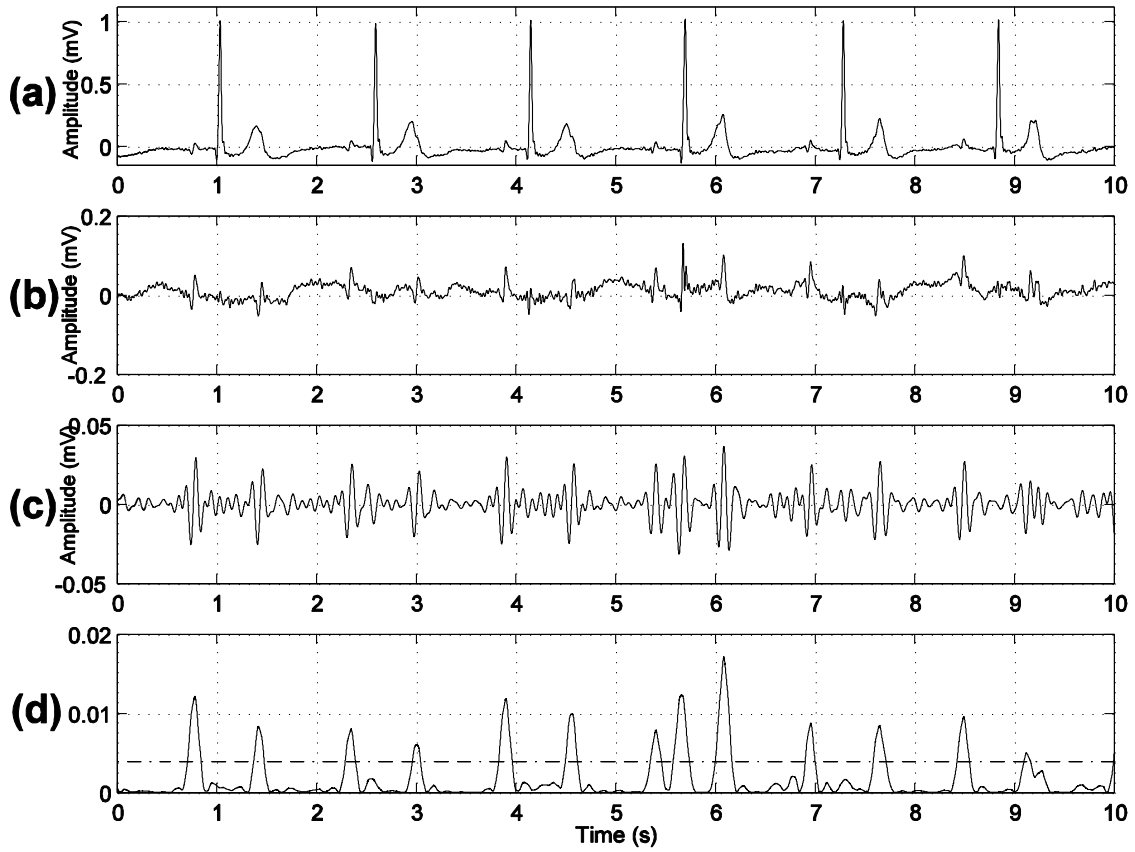

Figure 6. a) ECG. b) Residual signal (r(n)). c) Filtered residual signal (5-15Hz). d) ASNEO of c) with threshold (dotted line).

Determination of the location of P waves

Application of SNEO

After the filtering described in 4.1, the components of higher frequency in the filtered residual signal come mainly from the P waves. In our study, in order to highlight the existence of these waves from other components, a nonlinear operator was applied, the Nonlinear Energy Operator (NEO) proposed by Teager and Kaiser [14]. This operation has been used in the detection of spike-like signals because it is very sensitive to instantaneous changes in the energy signal that are frequency-dependant. With this method, the residues of T waves and other undesired components in the signal were minimized. However, since NEO is very sensitive to noise, (especially to high frequency noise), the Smoothed Nonlinear Energy Operator (SNEO), which uses a smoothing window, is usually applied. For a discrete signal, x(n), it is defined as [22]

$$\Psi[x(n)] = x^2(n) - x(n+1)\cdot x(n-1)$$

$$\Psi_S[x(n)] = \Psi[x(n)] \otimes w(n)$$

where Ψ is the NEO operator, Ψ_S the SNEO operator, $\otimes$ the convolution operator, and *w(n)* the smoothing window function. Finally, the absolute value of SNEO (ASNEO) was used. Figure 6d shows an example of the SNEO application on the filtered residual signal.

Determination of the detection threshold.

In order to detect the existence of P waves, a threshold was applied to ASNEO. The algorithm initializes the threshold and other internal parameters for each segment, which allows adaptation to changes in the characteristics of the signal. The aforementioned threshold was composed of two terms: the first term is a constant one that is related to an absolute threshold below which the signal is considered to contain only noise. The second term depends on the value of ASNEO in the current segment.

Due to the fact that QRS residues can generate extreme values in ASNEO, (which will increase the threshold and prevent the correct detection of P waves), the ASNEO values corresponding to the QRS residues were rejected during the calculation of this second term. To achieve this, the ASNEO sequence (in which the sections around the R mark were eliminated) creating the eSNEO signal:

$$\mathrm{eSNEO} = \mathrm{ASNEO} - \left\{\mathrm{ASNEO}\left[\mathrm{R_i} - \mathrm{vR}, \mathrm{R_i} + \mathrm{vR}\right]\right\},\ \mathrm{i} = 1...\mathrm{numR}$$

with *vR* being the rejected window in both sides of the R annotation, R_i being the annotation corresponding to the i-th R wave, and *numR* being the number of detected R. Finally, the expression used for the ASNEO threshold (TH_ASNEO) is:

$$\mathrm{TH\_ASNEO} = \mathrm{k_0} + \mathrm{k_1}.\mathrm{median}\left(\mathrm{eSNEO}\right)$$

The median was used because of its robustness in presence of outliers. Figure 6d shows the threshold calculated from eSNEO, superimposed on ASNEO.

Determination of the location of P waves

The procedure to determine the location of the P waves was the following: first, the values of ASNEO greater than *TH_ASNEO* were obtained. Next, the values that fulfill a separation criterion greater than a selected minimum value that is related to the minimum period between consecutive P waves (*tmin_P*) were selected. Finally, the maximum of the P wave detected by local search was marked (see Figure 7a).

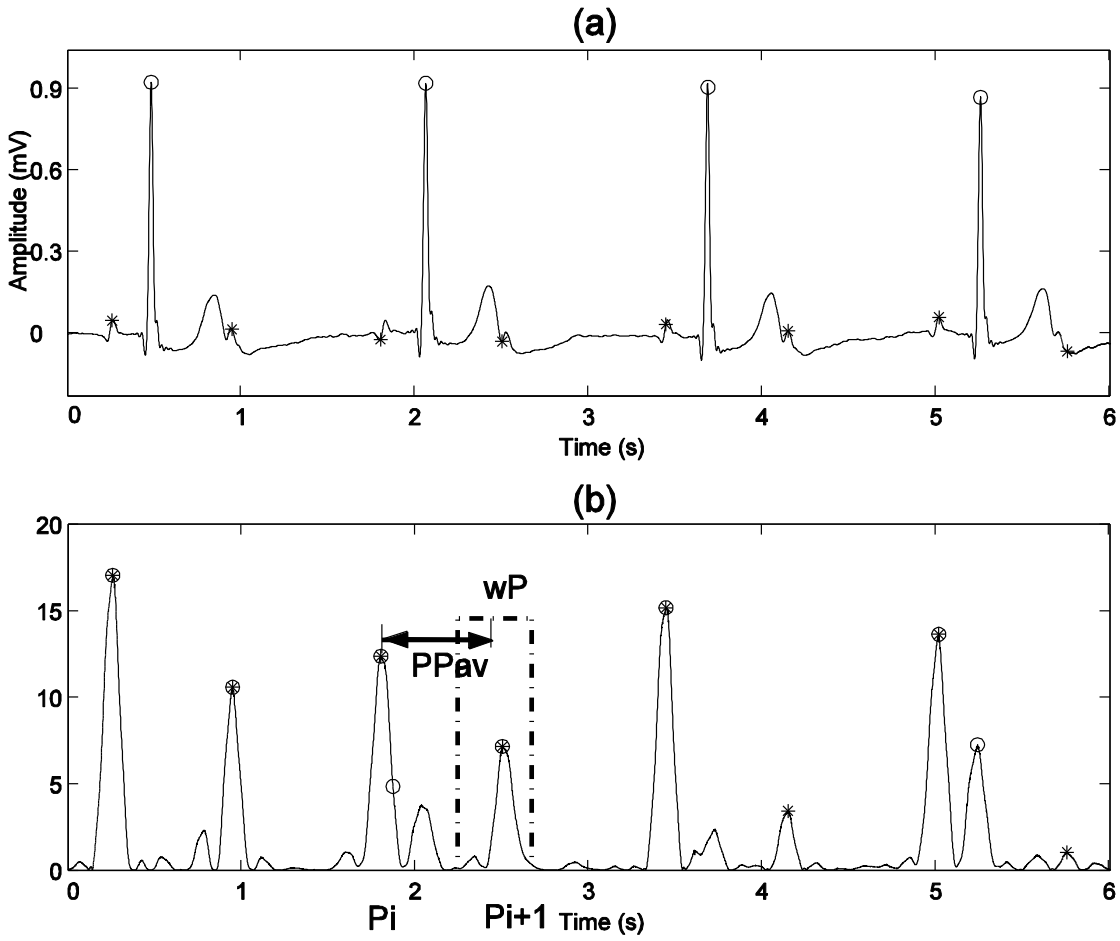

Figure 7. a) ECG. Circles indicate the location of R waves, and asterisks indicate the location of P waves. b) ASNEO. Circles indicate the locations of P waves before correcting the detection failures. Asterisks mark the final location of P waves after the correction. wP is the searching window for P_{i+1} (dotted line), and PP_{av} determines the relative position of the center of wP.

In order to correct the possible presence of false positives (FP: detection of nonexistent P waves) or false negatives (FN: lack of detection of real P waves), a criterion based on the normal rate between P waves was applied. The criterion verifies that each P wave is within a search window that is valid with respect to the last detected P. If the coupling is shorter than the expected one, a FP must be eliminated. If it is longer, a P wave has not been detected (FN) and a backwards search must be performed to locate it. The backwards search uses a reduced threshold to take into account the amplitude differences among P waves. This search was performed only once to avoid the detection of noise.

First, the searching window *wP* was determined (see Figure 7b). The center of the window was determined by the value of the coupling between valid P waves, PP_{av}. The width of the window was related to the maximum variation margin of the P wave coupling that is considered as valid, ΔPP. For the i-th P wave detected, the valid search window wP_i was defined as:

$$\mathrm{wP_i} = \left[\mathrm{P_i} + \left(1 - \Delta\mathrm{PP}\right).\mathrm{PP_{av}}, \mathrm{P_i} + \left(1 + \Delta\mathrm{PP}\right).\mathrm{PP_{av}} \right],\ \mathrm{i} = 1...\mathrm{numP}$$

The value of the coupling PP_{av} was initialized for every segment and it was updated after detecting a valid P wave. For the estimation of the initial value, the P waves that were overlapped with QRS residues were rejected with the same criterion as in the ASNEO threshold calculation. A subset (*eP*) was obtained, which was then used in the initialization of PP_{av}:

$$\mathrm{eP} = \left\{ \mathrm{P_k}, \text{if } \mathrm{P_k} \not\subset \left\{ \left[\mathrm{R_i} - \mathrm{vR}, \mathrm{R_i} + \mathrm{vR} \right] \right\},\ \mathrm{i} = 1...\mathrm{numR} \right\},\ \mathrm{k} = 1...\mathrm{numP}$$

where P_k is the i-th P wave detected, *eP* is the array resulting from the rejection of the P marks that are overlapped with R marks, and *numP* is the number of detected P waves. The initial value of PP_{av} was calculated as:

$$\mathrm{PP_{av}} = \mathrm{median}\left(\left\{ \mathrm{eP_{i+1}} - \mathrm{eP_i} \right\},\ \mathrm{i} = 1...\mathrm{num\_eP} - 1 \right)$$

with *num_eP* being the number of elements of *eP* array.The update of PP_{av} was given by:

$$PP_{av} = \begin{cases} k_{pp}.PP_{av} + (1 - k_{pp}).(P_{i+1} - P_i) & \text{, if } P_{i+1} \subset wP \\ PP_{av} & \text{, otherwise} \end{cases}$$

For each analyzed P wave, the following results were obtained:

1. P_i is in the wP search window: valid P wave (TP: true positive).
2. P_i is on the left of the wP search window: false detection (FP: false positive).
3. P_i is on the right of the wP search window: not detected P wave (FN: false negative). A backward search was activated once using a reduced threshold value (TH_ASNEO/4).

5. Results

Automatic evaluation of the QT cancellation process

An exhaustive search for the value of the adaptation constant (μ) between 0.002 and 0.2 with increments of 0.002 was conducted to find its optimal value. Two cancellation methods were tested:

1. Using the QT segment as cancellation pattern.
2. Performing a double cancellation. First, the QRS segment was cancelled (aligned with respect to QRS), then the T wave was cancelled (aligned with respect to the T wave).

In method 2, the QRS pulse had a length of *Lqrs*, and the T wave had a length defined by *Lt*; therefore, the total pulse length was the same in both cases.

To find the optimal value of μ, two estimators were used to quantify the cancellation degree. It is worth noting that the main error source detecting P waves after the cancellation process was due to the remaining

contribution of the QRS complex. As Figure 5c shows, a measure of the cancellation degree is the signal level in this area (see the signal inside the ovals). The defined estimators consist of calculating the signal mean power after the cancellation process:

i.- Mean power of the QRS complex residue, canceling QRS and T separately according to cancellation method 1: *res_qrs*.

ii.- Mean power of the QRS complex residue, canceling QT completely according to cancellation method 2: *res_pulse*.

For each tested value of the adaptation constant (μ), the estimators *res_qrs* and *res_pulse* and a copy of the obtained residual signal were saved. This way, the residual signals for each μ value allowed us to verify if the criterion was appropriate. The μ value that minimizes the power was selected as the optimum. The calculated values of *res_qrs* and *res_pulse* for each segment are shown in Figure 8. Figure 8a and Figure 8b show the *res_qrs* and *res_pulse* values obtained for all the records. Figure 8c and Figure 8d show the same values calculated for records 1 and 2. The optimal μ value was selected taking the minimum in these curves. Once the μ optimal value was determined, the algorithm was applied again with this value and the residual signal was obtained. This way each segment was filtered with the most suitable μ value.

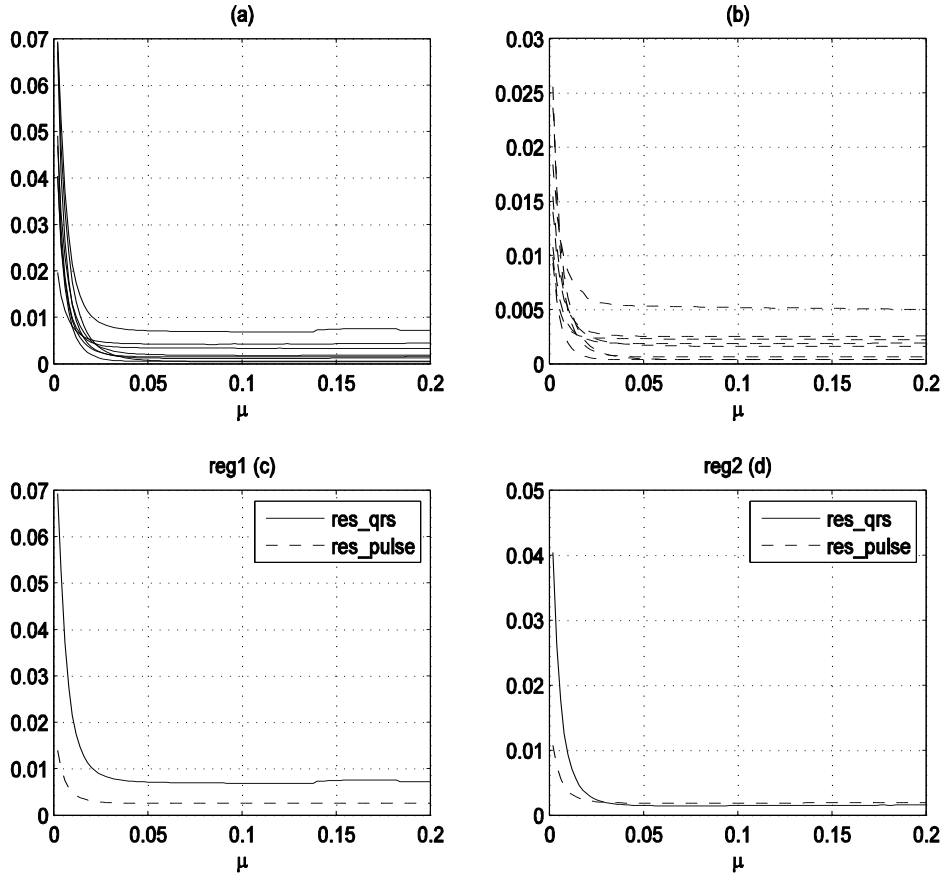

Figure 8. (a) and (b): Plot of res_qrs and res_pulse estimators in all records. (c) and (d): The same estimators for records 1 and 2.

We noticed that, for values of μ above 0.05, the error had few variations for all the records and the behaviors of both estimators were very similar.

Figure 9 shows the evolution of the optimal adaptation constant in a 24-hour record. Each μ value belonged to a record segment. We noticed that μ values outside the interval [0.05, 0.1] were due to noisy parts of the record where the QRS detection algorithm failed; thus, the cancellation process did not work correctly.

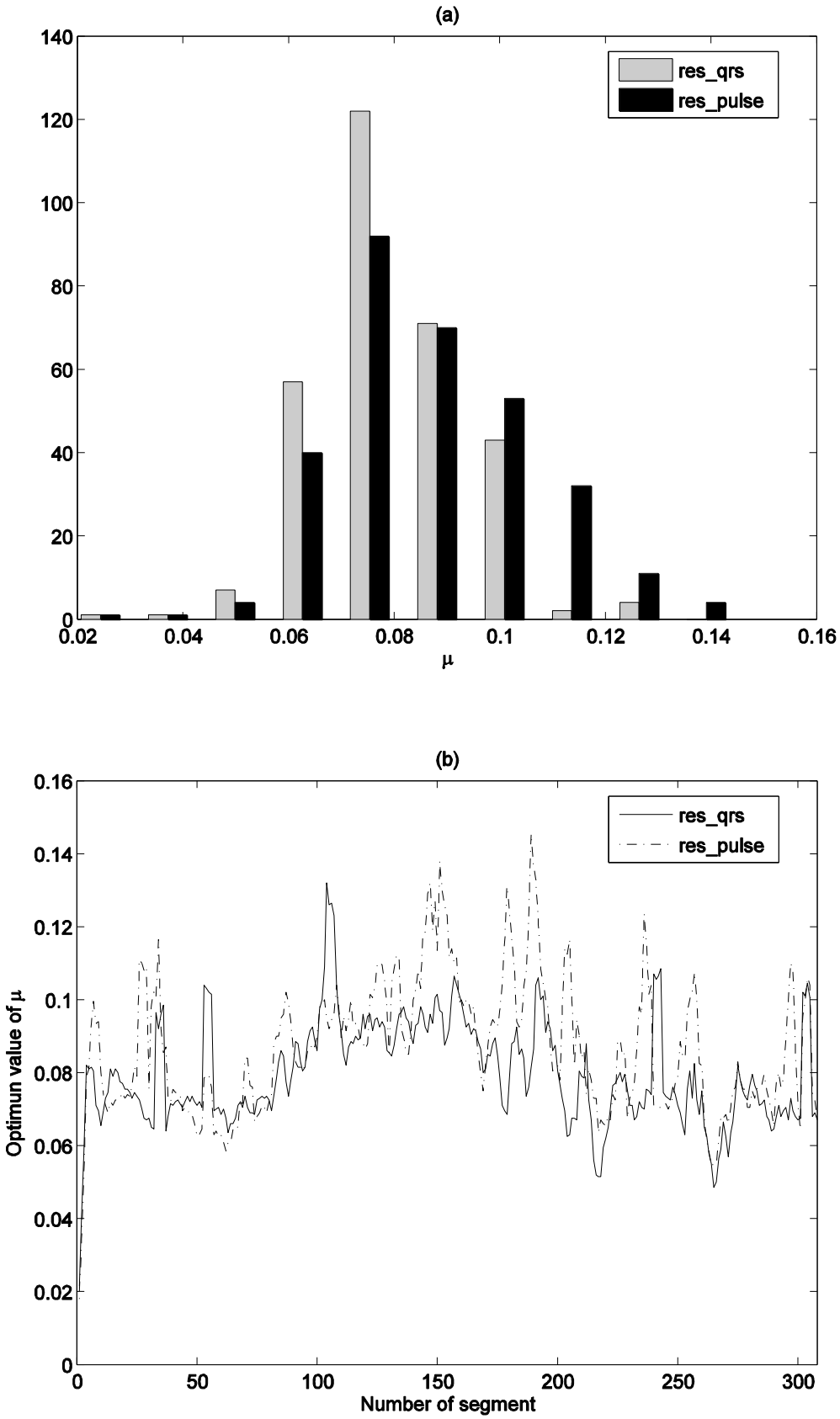

Figure 9.(a) Histogram of the optimal μ values in one record. (b) Evolution of μ through that record.

5.2. P wave detector

To obtain the reference marks for the record set used, a one-hour length section was selected randomly from each record. These sections were manually annotated by two experts separately. The absolute maximum of the R waves (N=16029) and the P waves (N=34892) were located and annotated. The sensitivity (S) and positive prediction (+P) were calculated to evaluate detector performance:

$$S = TP/(TP + TN)$$
$$+P = TP/(TP + FP)$$

where TP, FP and FN are the number of true positives (TP), false positives (FP) and false negatives (FN) detected by the algorithm.

To adjust the P wave detector parameters, an exhaustive search for these parameter values was performed over the training set of records, and the combination of values where the positive prediction (+P) was maximum, were selected. The maximum +P values were obtained for t_segm=180s, vR=45ms, k_0=6, k_1=3, k_{PP}=0.8, tmin_P=0.4s, ΔPP=0.2.

TABLE 1. Results for the P wave detector.

Record	# Detector	# Expert	TP	FP	FN	S (%)	+P (%)
Training set							
1	4844	4897	4508	336	389	92.06	93.06
2	4225	4279	4127	98	152	96.45	97.68
3	6778	7007	6270	508	737	89.48	92.51
4	3891	3837	3587	303	250	93.48	92.21
Mean:			**4623**	**311**	**382**	**92.87**	**93.87**
Test set							
5	3883	3856	2948	936	908	76.45	75.90
6	4193	4206	4098	95	108	97.43	97.73
7	3138	3130	2958	180	172	94.50	94.26
8	3674	3680	3103	571	577	84.32	84.46
Mean:			**3277**	**446**	**441**	**88.18**	**88.09**
Total mean:			**3950**	**378**	**412**	**90.52**	**90.98**

#Detector: number of detections by the algorithm. #Expert: number of detections by the expert. TP: true positives. FP: false positives. FN: false negatives. S: sensitivity. +P: positive prediction.

Table 1 shows final S and +P values for the training and test sets. All values were above 90% in spite of the specific difficulties of this pathology. The limitations of the developed detector can be explained taking

into account several factors. First, undetected R waves prevent the AICF and P wave detectors from working properly. In our study the R wave detector had mean results of S = 99.33% and +P = 98.39%. This indicates that the R detector works very well with normal R waves; however, it does not mark ectopic pulses as such, although the number of cases of this type is small in the set of records. Second, the AICF canceller can produce high residuals when canceling the QT segment, due mainly to two reasons: the first reason is related to the R detector errors, which are the reference entries to the AICF. The second reason is due to important variations in the morphology of the segment to be canceled. Some causes for morphologic variations are the presence of overlapping between the P wave and the QT segment, or variations in the pattern of the QT segment, which impedes an optimal cancellation.

Table 2 shows the results from Table 1 in accordance with the detected P waves. Two cases were taken into account for both sets of records: when the detected P wave was overlapped with the QRS residue, and when this overlapping was not present. Global values are also shown as reference. When overlapping existed, (which represented about 16% of the P waves in the set of records), an increase of false detections was observed, which decreased the corresponding values of S and +P.

TABLE 2. P Wave detection.

	#Detector	#Expert	S (%)	+P (%)
Training set				
Overlapped P-QRS	2943	2589	**74.67**	**59.36**
Non-overlapped P	16795	17431	**92.21**	**95.52**
All the cases	19738	20020	**92.87**	**93.87**
Test set				
Overlapped P-QRS	2423	1631	**68.52**	**50.71**
Non-overlapped P	12465	13241	**88.68**	**94.22**
All the cases	14888	14872	**88.18**	**88.09**
Total set				
Overlapped P-QRS	5366	4220	**71.59**	**55.04**
Non-overlapped P	29260	30672	**90.44**	**94.87**
All the cases	34626	34892	**90.52**	**90.98**

Number of P waves detected by the algorithm (#Detector) and by the expert (#Expert) in areas with and without overlapping between the P wave and the QRS residue. Results for S and +P are mean values over the training, test and total set of records.

The P wave detector was sensitive to the presence of QT segment residuals because they had high frequency components that were emphasized when SNEO was applied. The error correction of the algorithm, which is based on normal rhythm criteria, failed when the patient's P wave rhythm variability

presented strong variations pulse by pulse. When this occurs, the search window, which is located in accordance with the averaged previous rhythm, moves to incorrect positions, producing FP or FN.

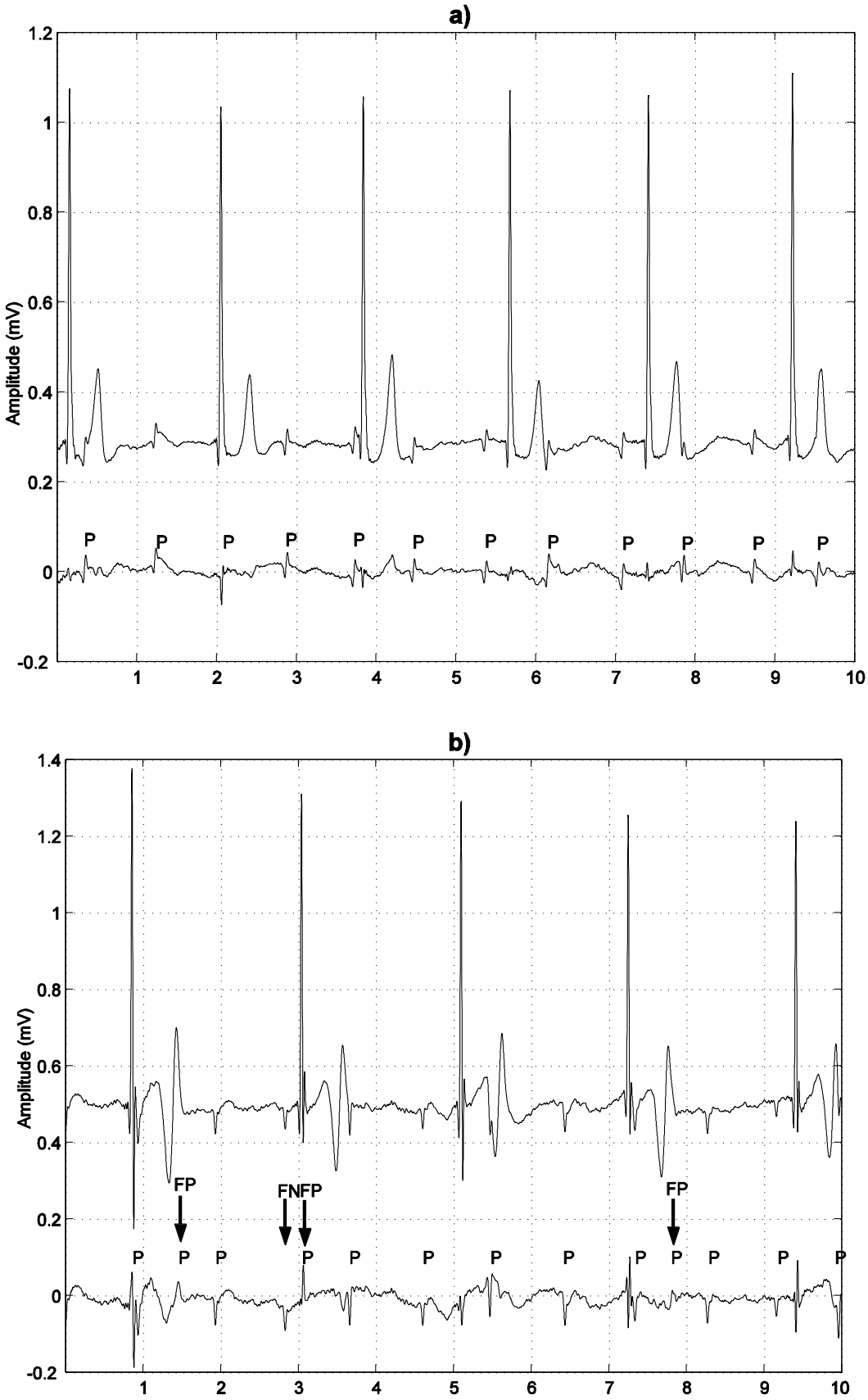

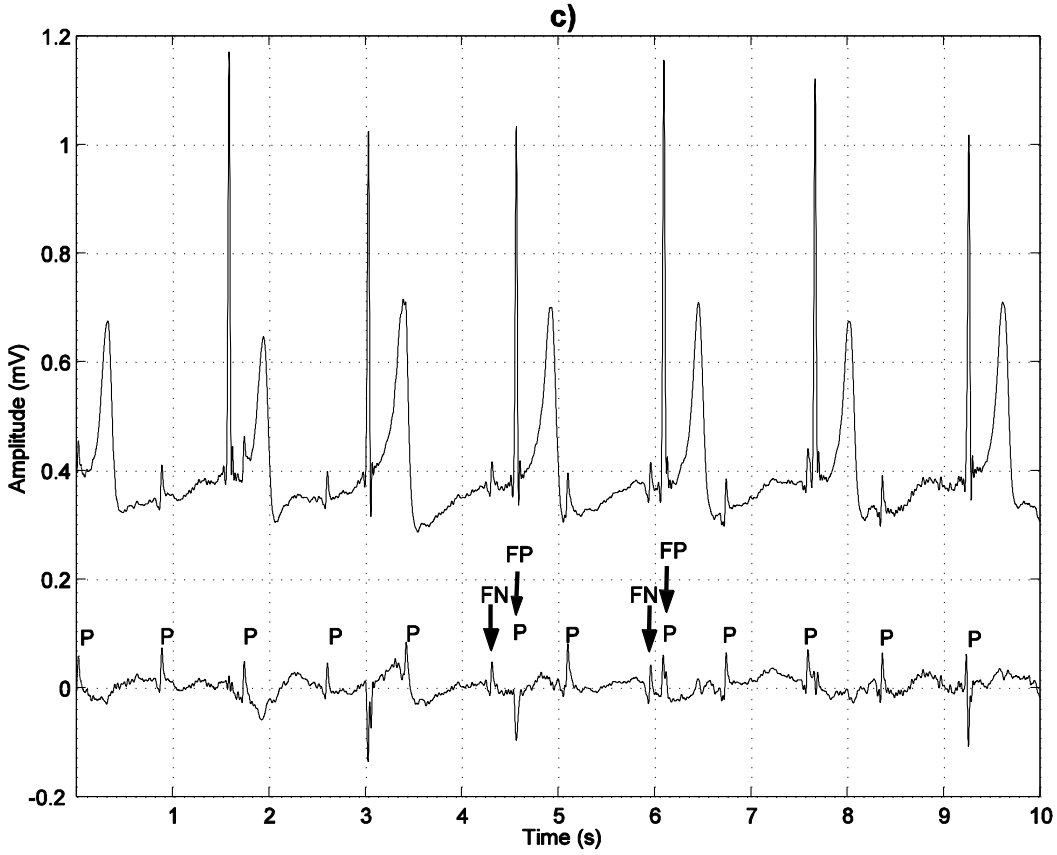

Figure 10. 10-seconds segments of some records used in this study: a) record 6, b) record 5, c) record 8. Upper trace: original signal; lower trace: residual signal. P waves detected by the algorithm are marked as reference. False positives or negatives are signaled by arrows.

Figure 10a shows a 10-second segment for record 6. This record gave the best results. The upper plot shows the original signal, and the bottom plot shows the residual signal after the QT segment cancellation. The QRS residues usually had low values and the number of overlappings with P waves was low, thus high accuracy was obtained. The algorithm was able to detect the presence of P waves overlapped with QRS complex (second 2) and T waves (second 9.5), which cannot be easily identified visually.

Figure 10b shows a 10-second segment for register 5. This record obtained the worst results. In this case, the morphology variations of the pattern to be canceled were high, thus the residues of QRS and T wave were detected as false P waves (FP). If a residue was detected and it was a real P wave inside the search window, this P wave was not detected, producing a double mistake.

Figure 10c shows a 10-second segment of record 8. Although some of the morphology variations of the pattern to be cancelled were not as important as the previous record, this record showed a large number of

overlappings between P waves and QRS segments. Arrows in the plot show the QRS residuals (marked as P: FP) near to the real P waves (seconds 4.2 and 6), which were not detected (FN).

Figure 11 shows an example of the RR and PP series obtained using the detector. Note the independence between them which is typical in this pathology: the PP rhythm is much slower than the atrial rhythm.

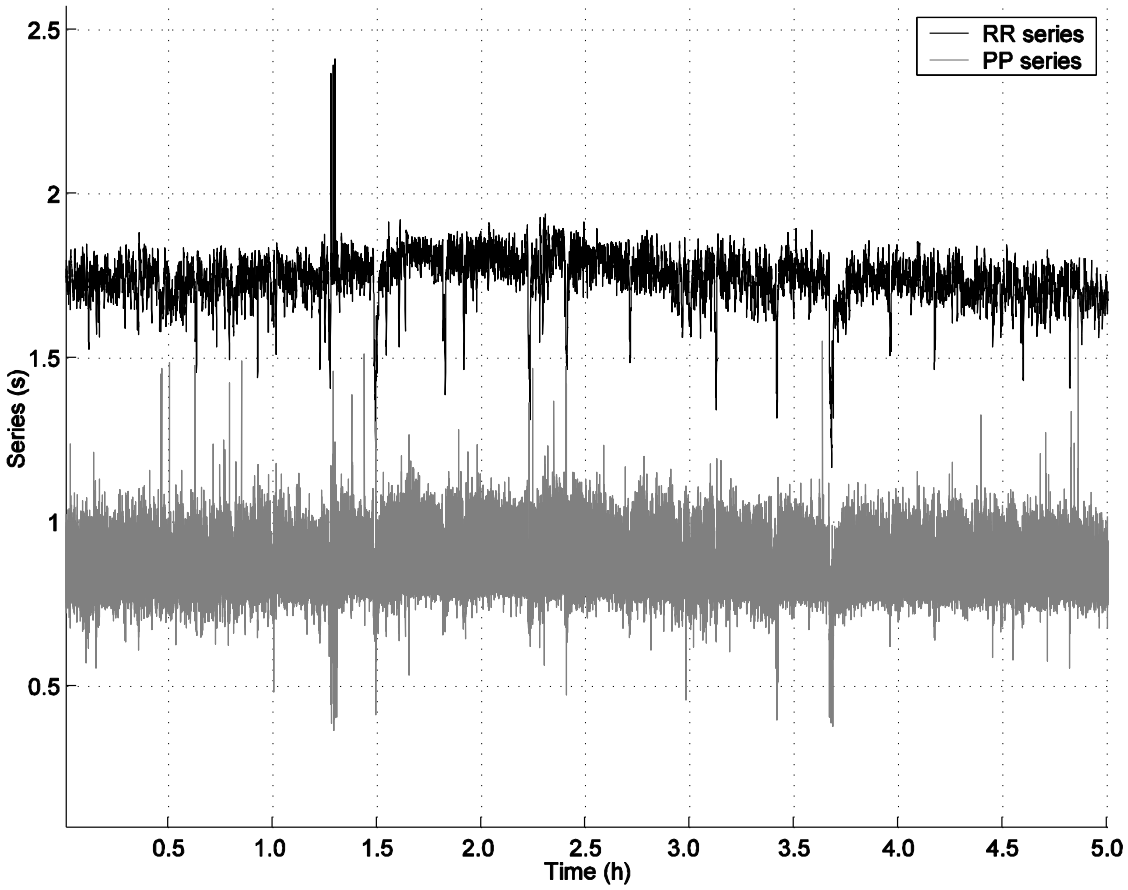

Figure 11. Temporal series: RR (top draw) and PP (bottom draw).

6. Conclusions

This work introduces a new algorithm for the detection of P waves in non-invasive ECG records from patients with type III AVB. In this pathology, P and R waves are not correlated; therefore, conventional P wave algorithms are not suitable. The adopted solution is based on the previous cancellation of the QT segment, and the P wave detection in the obtained residual signal. This approach has been previously tested on similar problems, like the fetal ECG detection in abdominal records.

The results of applying the algorithm for one-channel Holter records showed sensitivity and positive prediction mean values above 90%. These results were similar to other P wave detectors where the P wave and the QRS complex (or the T wave) were not overlapped. [10, 27]. The algorithm can be improved especially by reducing QT segment residues. The use of this detector in multichannel records, together with a decision algorithm, would reduce the number of false detections.

Finally, the developed algorithm obtains PP and RR series in type III AVB records, this permits the study of the atrial rate variability and its relationships with ventricular variability for this pathology.

Acknowledgements

We thank Dr. Ernesto Dallí from the Cardiology Service of Arnau de Vilanova Hospital (Valencia, Spain) for the selection of the records utilized in the study. The authors gratefully acknowledge the critical and helpful advice of the referees to make the paper more clear and concise.

References

1. Abboud, S., G. Barkai, S. Mashiach, and D. Sadeh. Quantification of the fetal electrocardiogram using averaging technique. Comput. Biol. Med. 20:147-155, 1990.

2. Almenar, V. and A. Albiol. A new adaptive scheme for ECG enhancement. Signal Process 75:253-263, 1999.

3. Chorro, F. J., J. F. Guerrero, J. Calpe, E. Dalli, M. Burguera, M. Bataller, P. Malo, J. Sanchis, J. Espí, and H. P. Lorenz. Variabilidad de la frecuencia cardíaca en el bloqueo A-V completo de origen congénito. Análisis espectral. Revista Latina de Cardiologia 16, 1995.

4. Ciaccio, E. J. and E. Micheli-Tzanakou. Development of gradient descent adaptive algorithms to remove common mode artifact for improvement of cardiovascular signal quality. Ann. Biomed. Eng. 35:1146-1155, 2007.

5. Clarkson, P. M. Optimal and Adaptive Signal Processing. : CRC Press, Inc., 1993, 529 pp.

6. Conover, M. Understanding Electrocardiography. : Mosby, 2002.

7. Ferrara, E. R. and B. Widrow. Fetal electrocardiogram enhancement by time-sequenced adaptive filtering. IEEE Trans. Biomed. Eng. 29:458-460, 1982.

8. Guerrero, J. F., M. Martinez, M. Bataller, and J. R. Magdalena. A new algorithm for foetal QRS detection in surface abdominal records. Computers in Cardiology 2006 33:441-444, 2006.

9. Hampton, J. R. The ECG made easy. Edinburgh etc.: Churchill Livingstone, 1998, 129 pp.

10. Hee-Kyo Joeng, Kwang-Keun Kim, Sun-Chul Hwang, and Myoung-Ho Lee. A new algorithm for P-wave detection in the ECG signal. Engineering in Medicine and Biology Society, 1989. Images of the Twenty-First Century. Proceedings of the Annual International Conference of the IEEE Engineering in :42-43 vol.1, 1989.

11. Hsiao, H. C., H. W. Chiu, S. C. Lee, T. Kao, H. Y. Chang, and C. W. Kong. Esophageal PP intervals for analysis of short-term heart rate variability in patients with atrioventricular block before and after insertion of a temporary ventricular inhibited pacemaker. Int. J. Cardiol. 64:271-276, 1998.

12. Jane, R., H. Rix, P. Caminal, and P. Laguna. Alignment methods for averaging of high-resolution cardiac signals: a comparative study of performance. IEEE Trans. Biomed. Eng. 38:571-579, 1991.

13. Jeras, M., R. Magjarevic, and E. Pacelat. Real Time P-Wave Detection in Surface Ecg. IFMBE Proceedings MEDICOM :405-408, 2001.

14. Kaiser, J. F. Some useful properties of Teager's energy operators. Acoustics, Speech, and Signal Processing, 1993. ICASSP-93. , 1993 IEEE International Conference on 3:149-152 vol.3, 1993.

15. Kim, K., Y. H. Lee, H. Kwon, J. M. Kim, I. S. Kim, and Y. K. Park. Averaging algorithm based on data statistics in magnetocardiography. Neurol. Clin. Neurophysiol. 2004:42, 2004.

16. Laguna, P., R. Jane, O. Meste, P. W. Poon, P. Caminal, H. Rix, and N. V. Thakor. Adaptive filter for event-related bioelectric signals using an impulse correlated reference input: comparison with signal averaging techniques. IEEE Trans. Biomed. Eng. 39:1032-1044, 1992.

17. Laguna, P., N. V. Thakor, P. Caminal, R. Jane, H. R. Yoon, A. Bayes de Luna, V. Marti, and J. Guindo. New algorithm for QT interval analysis in 24-hour Holter ECG: performance and applications. Med. Biol. Eng. Comput. 28:67-73, 1990.

18. Martinez, M., E. Soria, J. Calpe, J. F. Guerrero, and J. R. Magdalena. Application of the adaptive impulse correlated filter for recovering fetal electrocardiogram. Computers in Cardiology 1997 :9-12, 1997.

19. Michaelsson, M. and M. A. Engle. Congenital complete heart block: an international study of the natural history. Cardiovasc. Clin. 4:85-101, 1972.

20. Michaelsson, M., A. Jonzon, and T. Riesenfeld. Isolated congenital complete atrioventricular block in adult life. A prospective study. Circulation 92:442-449, 1995.

21. Motte, G., S. Dinanian, and C. Sebag. Classification and pitfalls of atrioventricular blocks. Arch. Mal. Coeur. Vaiss. 90 Spec No 1:47-55, 1997.

22. Mukhopadhyay, S. and G. C. Ray. A new interpretation of nonlinear energy operator and its efficacy in spike detection. IEEE Trans. Biomed. Eng. 45:180-187, 1998.

23. Pan, J. and W. J. Tompkins. A real-time QRS detection algorithm. IEEE Trans. Biomed. Eng. 32:230-236, 1985.

24. Park, M. K. and W. G. Guntheroth. How to read pediatric ECG's. : Mosby-Year Book Inc., 1992, 248 pp.

25. Sahambi, J. S., S. N. Tandon, and R. K. Bhatt. Using wavelet transforms for ECG characterization. An on-line digital signal processing system. IEEE Eng. Med. Biol. Mag. 16:77-83, 1997.

26. Shouldice, R., C. Heneghan, P. Nolan, and P. G. Nolan. PR and PP ECG intervals as indicators of autonomic nervous innervation of the cardiac sinoatrial and atrioventricular nodes. Neural Engineering, 2003. Conference Proceedings. First International IEEE EMBS Conference on :261-264, 2003.

27. Sternickel, K. Automatic pattern recognition in ECG time series. Comput. Methods Programs Biomed. 68:109-115, 2002.

28. Stridh, M. and L. Sornmo. Spatiotemporal QRST cancellation techniques for analysis of atrial fibrillation. IEEE Trans. Biomed. Eng. 48:105-111, 2001.

29. Thakor, N. V. and Y. S. Zhu. Applications of adaptive filtering to ECG analysis: noise cancellation and arrhythmia detection. IEEE Trans. Biomed. Eng. 38:785-794, 1991.

30. Van Alste, J. A. and T. S. Schilder. Removal of base-line wander and power-line interference from the ECG by an efficient FIR filter with a reduced number of taps. IEEE Trans. Biomed. Eng. 32:1052-1060, 1985.

31. Widrow, B., J. R. Glover Jr., J. M. McCool, J. Kaunitz, C. S. Williams, R. H. Hearn, J. R. Zeidler, J. Eugene Dong, and R. C. Goodlin. Adaptive noise cancelling: Principles and applications. Proceedings of the IEEE 63:1692-1716, 1975.

32. Zarzoso, V., A. K. Nandi, and E. Bacharakis. Maternal and foetal ECG separation using blind source separation methods. IMA J. Math. Appl. Med. Biol. 14:207-225, 1997.